Available online at www.sciencedirect.com
ScienceDirect
Journal of Catalysis 250 (2007) 195–208
JOURNAL OF CATALYSIS
www.elsevier.com/locate/jcat

Pt/Ga_2O_3 catalysts of selective hydrogenation of crotonaldehyde

E. Gebauer-Henke [a], J. Grams [a], E. Szubiakiewicz [a], J. Farbotko [a], R. Touroude [b], J. Rynkowski [a,*]

[a] *Institute of General and Ecological Chemistry, Technical University of Łódź, ul. Żeromskiego 116, 90-924 Łódź, Poland*
[b] *LMSPC, UMR 7515 du CNRS, ECPM-ULP, 25 rue Becquerel, 67087 Strasbourg Cedex 2, France*

Received 27 February 2007; revised 11 June 2007; accepted 17 June 2007

Available online 27 July 2007

Abstract

Hydrogenation of crotonaldehyde in a gas phase at atmospheric pressure over Pt/Ga_2O_3 catalysts was studied. Two types of platinum precursors [$Pt(acac)_2$ and H_2PtCl_6] and two gallia supports (α-Ga_2O_3 [60.7 m^2/g] and β-Ga_2O_3 [2.2 m^2/g]) were used for catalyst preparation. The catalyst 5 wt% Pt/α-Ga_2O_3 prepared from $Pt(acac)_2$ precursor showed very high and stable selectivity to crotyl alcohol (91% and 63% at 10% and 70% crotonaldehyde conversion, respectively). Because Pt-supported catalysts, showing a high selectivity, usually have relatively low activity, the most interesting finding of this study is that the use of gallium oxide as a support for platinum makes it possible to obtain catalysts with significantly increased C=O bond hydrogenation selectivity while maintaining high activity.

Keywords: Platinum; Selective hydrogenation; Crotonaldehyde; Gallium oxide; Unsaturated alcohol

1. Introduction

Selective hydrogenation of α,β-unsaturated aldehydes to unsaturated alcohols has been a subject of many investigations because of its great interest as an important step in the preparation of various fine chemicals and applications of unsaturated alcohols in the flavor and fragrance industries and in pharmaceutical manufacturing [1]. The challenge lies in the selective hydrogenation of the carbonyl bond while keeping the olefinic bond unaffected. This can be achieved using stoichiometric amounts of reducing agents, such as hydrides (e.g., $AlLiH_4$, $NaBH_4$); however, such methods are useful only for a small-scale production because they involve costly chemicals and are hazardous to the environment.

The development of specific catalytic hydrogenation processes can replace the reduction using metal hydrides, which is in agreement with one of the 12 principles of green chemistry: "Catalytic reagents (as selective as possible) are superior to stoichiometric reagents." Catalysis offers advantages over stoichiometric reactions in terms of both increased selectivity and energy minimization. The specificity of catalysts favors the reaction to a preferred product, whereas the amount of undesired products is decreased. The amount of energy required for a given transformation is also reduced as the catalysts decrease the activation energy of the reaction [2]. Consequently, hydrogenation processes based on heterogeneous catalysis have been developed [3]. Hydrogenation of α,β-unsaturated aldehydes to unsaturated alcohols is difficult to realize, especially under heterogeneous catalysis conditions, due to the much greater susceptibility to hydrogenation of the C=C double bond (578.8 kJ/mol) compared with the C=O double bond (705.8 kJ/mol) for both thermodynamic and kinetic reasons [4].

The reaction of hydrogenation of α,β-unsaturated aldehydes may occur in different ways, as shown in Fig. 1. α,β-Unsaturated aldehydes may be hydrogenated to the most desired product, unsaturated alcohols (step 1), as well as to other saturated products, butanal (steps 2 and 5) and butanol (steps 3 and 4).

The selectivity to unsaturated alcohols depends on various factors, such as the structure of aldehydes, the nature of catalysts, and the presence of additives, as well as the reaction conditions [5]. Previous studies have shown that unpromoted metals have specific selectivities to unsaturated alcohols. For example, iridium and osmium are rather selective; palladium, rhodium, and nickel are unselective or slightly selective; and

* Corresponding author. Fax: +48 42 631 31 28.
E-mail address: jacryn@p.lodz.pl (J. Rynkowski).

0021-9517/$ – see front matter
doi:10.1016/j.jcat.2007.06.021

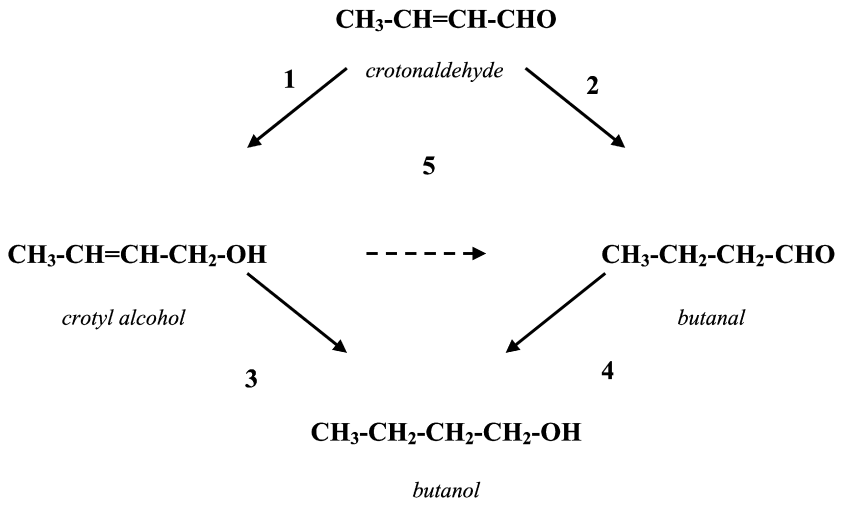

Fig. 1. Selective hydrogenation of crotonaldehyde: catalytic pathways.

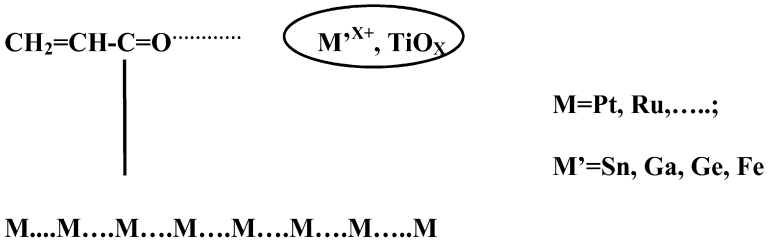

Fig. 2. Reaction sites for hydrogenation of α,β-unsaturated aldehydes on metallic-promoted catalysts [24].

platinum, ruthenium and cobalt are moderately selective. These trends were confirmed by Cordier for cinnamaldehyde hydrogenation (Os > Ir > Pt > Ru > Rh > Pd) [6]. Different geometric and electronic properties of metals can affect hydrogenation activities and selectivities by influencing not only adsorption, but also surface reactions. The adsorption phenomenon itself is limited by many factors, such as the mode of reactant adsorption on a specific metal surface. Different crystal phases of metals have different geometrical constraints, which explains the need to study the performance of distinct crystallographic faces. Platinum has been used most intensively as an active metal in chemoselective hydrogenations. Among the nonnoble metals, special attention has been given to the supported cobalt catalysts. This approach, which was initiated by Japanese scientists [7–10], was developed in the works of Hutchings et al. [11–13], Rodrigues and Bueno [14–16], and in our previous paper [17]. Recently, interesting properties of bimetallic Pt-Co/SiO_2 were reported by Borgna et al. [18]. Nonetheless, systems based on platinum are still the most frequently explored catalysts of crotonaldehyde hydrogenation. Pt is a very active metal in the hydrogenation of the C=C double bond but is not intrinsically selective to unsaturated alcohols. The selectivity to the desired product greatly depends on the steric and electronic structure of the active phase and reactant [19].

Enhanced selectivity can be obtained by an increase in C=O bond activity, with a simultaneous decrease in C=C bond activity. This can be achieved by using various promoters, which were divided into three groups: (a) alkali metal (Na, K, La, Ca, Cd) ionic compounds, (b) transition metal (Ti, V, Cr, Mn, Fe) compounds, and (c) nontransition element (Ge, Ga, Sn) compounds, with an increased promoting effect in the order (a) < (b) < (c) [20].

Earlier work [21,22] has shown the role and effects of promoters and metal–support interaction in the reaction of hydrogenation of α,β-unsaturated aldehydes. As a general rule, activity and selectivity to unsaturated alcohols are improved when adding Sn, Ge, Ga, Fe, and others to active transitional metals (e.g., Pt, Ru, Ni) and when a partially reducible support like TiO_2 is used [23]. The promoting effect is seen as a strong interaction between the carbonyl group and a positively charged center (e.g., $Fe^{\delta+}$, $Sn^{\delta+}$, $TiO_x^{\delta+}$) (Fig. 2) [24].

Gallium has been mentioned as an effective promoter in the reduction of carbonyl group in Pt-based catalysts [5]. Englisch et al. [22] showed that transitional metals like Ga can be used as promoters in catalysis for selective hydrogenation of α,β-unsaturated aldehydes. Transition metals used in catalysts have partially filled d-orbitals. When the platinum d-orbital is filled, the metal is relatively catalytically inactive, as in the cases of silver, gold, and copper. The interstitial electron densities in metals filling d-orbitals are low, and these metals are not eager to form bonds. However, the electronic structure of metal can be changed by adding a second metal, leading to, for instance, the formation of an alloy, by changing the metal particle size and enhancing the interaction with the support. This interaction decreases electron density at the carbonyl bond of α,β-unsaturated aldehyde and increases its reactivity. The re-

duction to unsaturated alcohol occurs if the sorption of the C=O group occurs at the Pt–gallium oxide interface, where the carbonyl group can be activated by Lewis acid sites and dissociated hydrogen can be supplied by Pt.

Based on the literature [25] and our preliminary studies, we suggest that Ga_2O_3 should be considered a partly reducible oxide of potential usefulness as a catalyst support. Consequently, it seemed interesting to test the catalytic properties of Pt/Ga_2O_3 systems in the reaction of selective hydrogenation of crotonaldehyde, never before studied in this context. The aim of this work was to determine the physicochemical characterization and catalytic performance of Pt/Ga_2O_3 systems in the reaction of crotonaldehyde hydrogenation in a gas phase.

2. Experimental

2.1. Support preparation

Two gallium oxide supports were used: α-Ga_2O_3 $S_{BET} = 60.7\ m^2/g$, mesoporous and β-Ga_2O_3 (Aldrich 21506-6, 99.99%, $S_{BET} = 2.2\ m^2/g$, nonporous). α-Ga_2O_3 was prepared in our laboratory by dissolving metallic gallium in concentrated nitric acid (V), followed by precipitation of $Ga(OH)_3$ with NH_3 aq., drying at 120 °C, and calcination at 500 °C for 3 h in air. The polymorphic forms of supports were determined by XRD.

2.2. Catalyst preparation

Pt/Ga_2O_3 catalysts were prepared by a wet-impregnation method of α- and β-Ga_2O_3, using an aqueous solution of hexachloroplatinic acid (H_2PtCl_6; P.O. Ch Gliwice, Poland) and a methanolic solution of platinum acetyl acetate [$Pt(acac)_2$; Aldrich]. Water and methanol were evaporated slowly on a hot plate. The samples were dried at 120 °C for 2 h and then calcined in air at 200 °C for 2 h.

The composition of catalysts and other abbreviations are presented in Table 1 (α and β, polymorphs of gallium oxide; A, platinum acetylacetonate; H, hexachloroplatinic acid; 5, 2, 1, and 0.5, percentages of the active phase). Atomic absorption spectroscopy (AAS) (at CNRS, Vernaison, France) and inductively coupled plasma (ICP) analyses were performed on calcined samples to evaluate metal loadings.

Table 1
Catalysts composition

Catalysts	Symbols	Pt precursors	Pt conc. (wt%)	Cl conc. (wt%)
5 wt% Pt/α-Ga_2O_3	α5A	$Pt(acac)_2$	5.16[a]	–
5 wt% Pt/β-Ga_2O_3	β5A	$Pt(acac)_2$	4.79[a]	–
5 wt% Pt/α-Ga_2O_3	α5H	H_2PtCl_6	5.25[a]	1.31
5 wt% Pt/α-Ga_2O_3	β5H	H_2PtCl_6	5.38[a]	<0.2
2 wt% Pt/α-Ga_2O_3	α2A	$Pt(acac)_2$	1.97[b]	–
2 wt% Pt/α-Ga_2O_3	β2A	$Pt(acac)_2$	1.87[b]	–
1 wt% Pt/α-Ga_2O_3	α1A	$Pt(acac)_2$	0.97[b]	–
1 wt% Pt/α-Ga_2O_3	β1A	$Pt(acac)_2$	0.99[b]	–
0.5 wt% Pt/α-Ga_2O_3	α0.5A	$Pt(acac)_2$	0.49[b]	–
0.5 wt% Pt/α-Ga_2O_3	β0.5A	$Pt(acac)_2$	0.47[b]	–

[a] AAS analysis.
[b] ICP analysis.

2.3. Catalytic tests

Catalytic tests were carried out in a glass reactor, operating at atmospheric pressure. The total gas flow controlled by a flowmeter varied with the changes in the pump rate at the end of the flow line. Pure crotonaldehyde (Fluka), stored in argon, was used as received. A specific quantity (50–250 μL) was drawn up from the bottle using a tight syringe and introduced through a vaccine cap into a reservoir installed online and maintained at 0 °C: therefore, aldehyde at constant partial pressure (8 Torr) was carried over the catalyst by hydrogen flow (50–60 cc/min). Beyond the aldehyde reservoir, the gas line was thermostatted at about 60 °C to avoid any condensation. The reaction products were drawn off of the flow line at different times during the catalytic run and analyzed by gas chromatography at 85 °C, using a flame ionization detector.

Catalyst samples (5–100 mg) were reduced in situ at 100, 200, or 300 °C for 1 h and cooled under H_2 before the reaction carried out at 50 and 80 °C.

The reaction activities were calculated using the formula $A = \alpha F/\omega$, where α is the crotonaldehyde conversion (in %), F is the flow rate of crotonaldehyde (in mol/s), and ω is the weight of platinum (in g). The selectivity to different products (crotyl alcohol, butanal, butanol, and hydrocarbons) was calculated as the molar ratio of the selected product to the total amount of products formed. The sensitivity factors are taken as 1.4 for the hydrocarbons and 1 for the other products.

It was checked that both supports alone, α- and β-Ga_2O_3, after H_2 pretreatment up to 300 °C, had no activity in crotonaldehyde hydrogenation.

2.4. Nitrogen adsorption (BET) measurements

BET surface areas and total pore volume for all catalysts and supports were obtained using a Sorptomatic 1900 (Carlo Erba Instruments), after heating the samples at 200 °C under vacuum.

2.5. TG–DTA–MS measurements

A thermogravimetric (TG) analyzer, equipped with a differential thermal analysis (DTA) device (Seteram SETSYS-16/18) and combined inline with a quadrupole mass spectrometer (MS) (Thermostar, Balzers) were used for the temperature-programmed reduction of the catalyst active-phase precursor. The TG–DTA–MS measurements were carried out with a ca. 20 mg sample, at a linear temperature increase of 10 °C per minute to a temperature range of 25–1100 °C.

2.6. XRD measurements

XRD analyses were carried out in Siemens D 5000 polycrystalline diffractometer using Cu$K\alpha$ radiation and X'PERT PRO MPD PAN polycrystalline diffractometer. Patterns of supports

were recorded in the scanning mode (2.0 s/step, step size: 0.05° 2θ, 2θ range 20°–100°). Spectra of the catalysts (after calcination at 200 °C) were recorded in the same scanning mode but in a 2θ range of 38°–48.5° (the region characteristic of for Pt, PtO_x, and some lines characteristic of α- and β-Ga_2O_3).

The mean crystallite size of Ga_2O_3 samples was related to a pure X-ray broadening by Scherer's formula, $D = k\lambda/\beta\cos\theta$. The measured line broadening b was corrected for the instrumental broadening B, using the equation $\beta = \sqrt{B^2 - b^2}$. The particle shape factor k was taken as 0.9. Phase identification was made based on JCPDS files.

2.7. TPR measurements

All TPR measurements were performed on an Altamira apparatus using an Ar–H_2 mixture (5 vol% H_2) and a flow rate of 50 cc/min, at a temperature ramp rate of 10 °/min. Before TPR, the samples (100 mg) were calcined in air at 200 °C for 2 h.

2.8. ToF-SIMS measurements

The ToF-SIMS investigations (α5A, β5A and α2A, β2A) were performed in the static mode using an ION–TOF instrument (TOF SIMS IV) equipped with a 25-kV pulsed $^{69}Ga^+$ primary ion gun. To obtain the plain surface of catalysts, powder samples were tableted before the measurements. For both catalyst samples, five spectra were collected (from different areas) to determine the distribution of Pt on the support. The $^{195}Pt^-/^{71}GaO^-$ and $^{35}Cl^-/OH^-$ intensity ratios were calculated.

2.9. TEM

High-resolution TEM images were recorded on a TOPCOM 002B electron microscope, operating at 200 kV, with a point-to-point resolution of 0.18 nm. Some catalyst grains obtained after different catalytic pretreatments performed in the catalytic apparatus were ground and diluted in an ethanolic solution. One drop of this solution previously dispersed in an ultrasonic tank, was deposited onto a Cu grid coated by a holed carbon film and dried in air. Various regions of the grid were observed and particle sizes were measured from the observation of 250–350 particles. The following formula was used to calculate the mean surface diameter: $ds = \sum n_i d_i^3 / \sum n_i d_i^2$, where n_i is the number of particles of diameter d_i.

2.10. FTIR measurements

FTIR measurements were obtained with a Shimadzu 8501 spectrometer using a quartz cell fitted with NaCl windows and an external furnace. Catalyst samples (80 mg) were prepared in the form of 25-mm-diameter discs. After the reduction in hydrogen at 300 °C, the cell was evacuated for 30 min at room temperature. Pulses of CO or crotonaldehyde were introduced at 25 °C, and spectra were recorded.

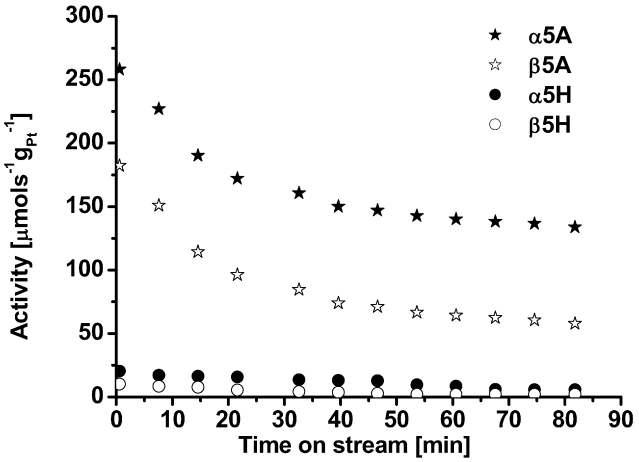

Fig. 3. Activity versus time on stream for 5 wt% Pt/Ga_2O_3 (temp. red. = 300 °C, temp. reaction = 80 °C, conv. < 20%).

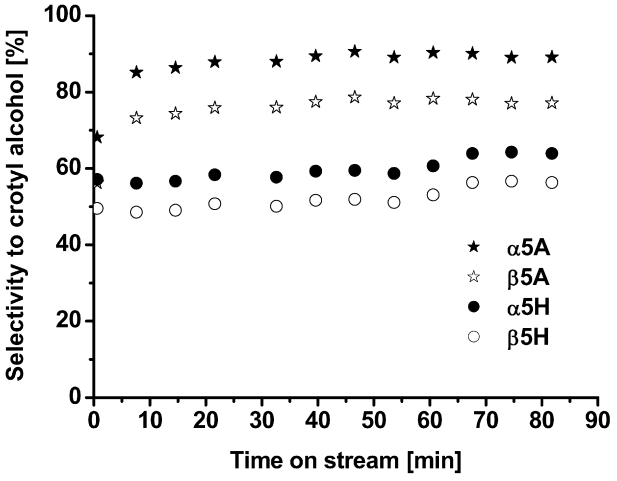

Fig. 4. Selectivity versus time on stream for 5 wt% Pt/Ga_2O_3 (temp. red. = 300 °C, temp. reaction = 80 °C, conv. < 20%).

3. Results and discussion

3.1. Catalytic tests

Detailed studies of the reaction of crotonaldehyde hydrogenation in a gas phase were carried out to determine the influence of polymorphic form of the support (gallium oxide [α, β]), platinum precursor [$Pt(acac)_2$, H_2PtCl_6], catalyst reduction temperature, reaction temperature, and platinum loading on the catalytic performance of the Ga_2O_3-supported Pt catalysts under study. For most of the catalysts, we checked the catalytic performance at 180 min time on stream. We found that after 40–60 min, the activity did not change and remained stable. That is why for all of the catalytic data presented in this paper, we limited the time on stream axis to 90 min.

Figs. 3 and 4 show the activity and selectivity of the 5 wt% Pt/Ga_2O_3 catalysts, illustrating the influence of different gallia polymorphs and catalyst precursors. During the first 45 min of time on stream, decreased activity can be seen, but subsequently the reaction reached a quasi-steady state. This effect is espe-

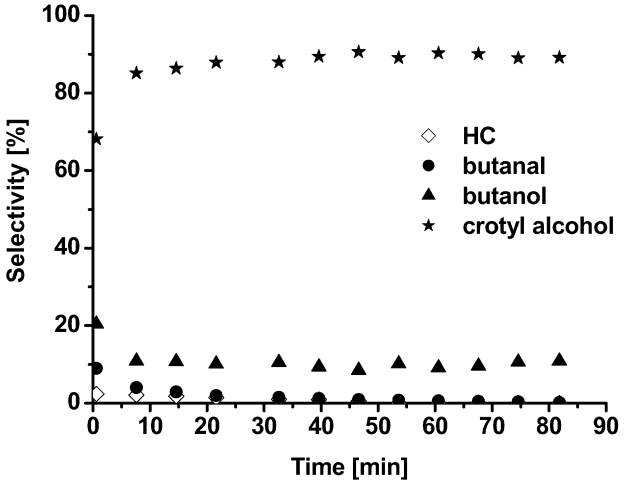

Fig. 5. Selectivity versus time on stream for α5A catalyst (temp. red. = 300 °C, temp. reaction = 80 °C, conv. < 20%).

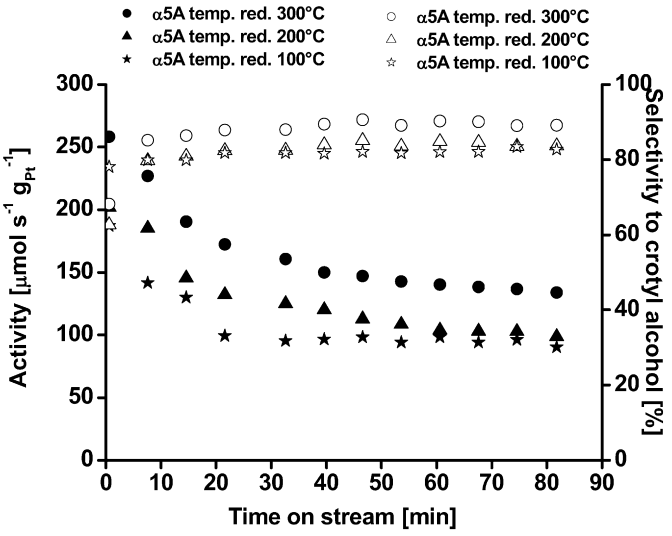

Fig. 6. Activity and selectivity versus time on stream for α5A catalyst, reduced at different temperature (temp. reaction = 80 °C, conv. < 20%).

cially clearly observed for the most active catalysts obtained from the $Pt(acac)_2$ precursor. The activity of the catalysts prepared from the chlorine-containing catalyst H_2PtCl_6 was poor. According to previous work [26–31], the presence of chlorine in the precursor can have a significant and diverse affect on the properties of the catalysts. For example, Pt/ZnO catalysts obtained using H_2PtCl_6 solution show better selectivity to desired crotyl alcohol than those prepared from $Pt(NO_3)_2(NH_3)_4$ [26,27], whereas the opposite is true for Pt/SnO_2 catalysts [28]. A more detailed discussion of the effect of residual chloride in the chemoselective hydrogenation of unsaturated aldehydes has been provided by Mäki-Arvela et al. [19].

Our catalysts prepared from H_2PtCl_6 were also relatively selective to crotyl alcohol (63% at the activity 2.4 $\mu mol\, s^{-1}\, g_{Pt}^{-1}$), but their much worse catalytic performance compared with that obtained from $Pt(acac)_2$, made us focus our attention on further studies concerning $Pt(acac)_2$ as a precursor. Fig. 5 shows changes of selectivity to the main products. After the first 50 min, the reaction reached a quasi-stable state. The significantly increased selectivity to crotyl alcohol accompanied by the decreased selectivity to butanol and butanal can be clearly observed during the first 10 min of the reaction.

In parallel, the activity dropped significantly, although this process is more extended (Fig. 3). This may suggest that at the beginning of the reaction, the most active centers on which the C=C double-bond hydrogenation predominates were suppressed, resulting in decreased activity but increased selectivity to crotyl alcohol.

Catalysts supported on α-Ga_2O_3 show significantly higher activity and selectivity compared with those supported on β-Ga_2O_3. This may connected with a much greater specific surface area of α-Ga_2O_3 compared with β-Ga_2O_3, leading to a difference in platinum particles size (3.5 nm on α-Ga_2O_3 vs 10.9 nm on β-Ga_2O_3).

The catalyst reduction temperature, especially in the case of catalysts supported on reducible supports exhibiting the SMSI effect, can influence the catalytic properties to a great extent. Before the reaction, the catalysts were reduced in situ at 100, 200, or 300 °C. As an example, the effect of the reduction temperature on the catalytic activity and selectivity of the most active catalyst α5A is presented in Fig. 6.

For all of the catalysts investigated in this work, the best catalytic performance was obtained for the samples reduced at 300 °C. The comparison of activity and selectivity in the reaction of crotonaldehyde hydrogenation for all of the investigated catalysts reduced at 100 and 300 °C is presented in Table 2. All values in this table are related to the steady state of the reaction for conversion <20%.

The abatement of the reaction temperature below 80 °C results in decreased activity (as can be expected) as well as in selectivity to crotyl alcohol to a certain extent. An example of the efficiency of catalysts α5A and β5A for the reaction carried out at 50 and 80 °C is presented in Fig. 7.

Up to now, all catalytic results have been reported for conversions <20% (usually ca. 10%) in all cases. Proper experimental parameters ensuring low conversions were chosen to limit the effects leading to the formation of a completely hydrogenated product, butanol. However, it is noteworthy that most of the catalysts supported on gallia studied in this work showed very high selectivity to crotyl alcohol up to 70% conversion. Fig. 8 illustrates the dependence of selectivity as a function of conversion for the most active catalyst, α5A. The data were taken at the steady-state regime. Considering the extremely high catalytic activity of this catalyst, such results are remarkable.

To sum up the catalytical studies, we can conclude that gallia-supported platinum catalysts, prepared from platinum acetylacetonate as a precursor, showed good performance in the reaction of selective hydrogenation of crotonaldehyde. The optimum parameters are the temperature of catalyst reduction (300 °C) and the temperature of reaction (80 °C). The 5 wt% Pt/α-Ga_2O_3 catalyst (α5A) showed the best catalytic properties, but lower-loaded catalysts containing 1 and 2 wt% of platinum showed promising catalytic performance as well (Table 2).

Table 2
Hydrogenation of crotonaldehyde on Pt/Ga_2O_3 catalysts at 80 °C

Catalysts	Reduction temperature									
	100 °C					300 °C				
	Act.	Selectivity (%)				Act.	Selectivity (%)			
		HC	Butanal	Butanol	CROTOL		HC	Butanal	Butanol	CROTOL
α5A	109	1	8	8	83	159	2	4	5	89
β5A	50	2	11	8	79	75	2	8	10	80
α5H	3	3	7	29	61	8	3	14	20	63
β5H	2	2	10	30	58	2	4	13	24	59
α2A	78	2	15	20	63	100	2	4	25	69
β2A	72	3	12	28	57	80	5	9	24	62
α1A	67	1	26	23	50	70	1	20	28	51
β1A	65	1	31	23	45	70	1	25	24	50
α0.5A	58	–	27	30	43	60	–	19	33	48
β0.5A	55	–	36	25	39	61	–	31	27	42

Note. Act.—activity (μmol s^{-1} g_{Pt}^{-1}). HC—hydrocarbons. CROTOL—crotyl alcohol.

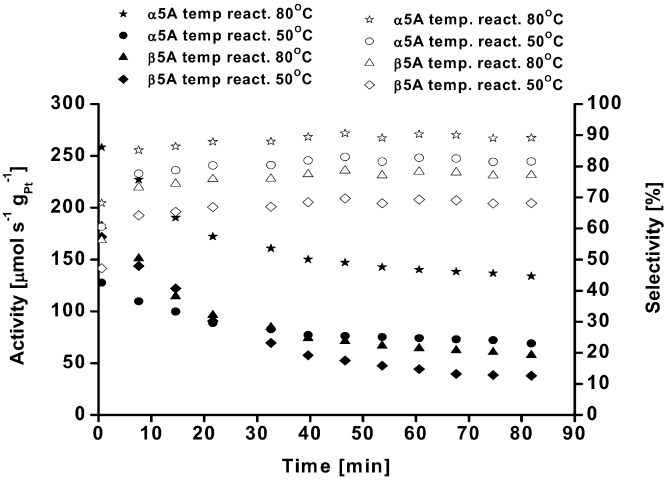

Fig. 7. Activity (full symbols) and selectivity to crotyl alcohol (empty symbols) for α5A and β5A catalysts after reduction at 300 °C (conv. < 20%).

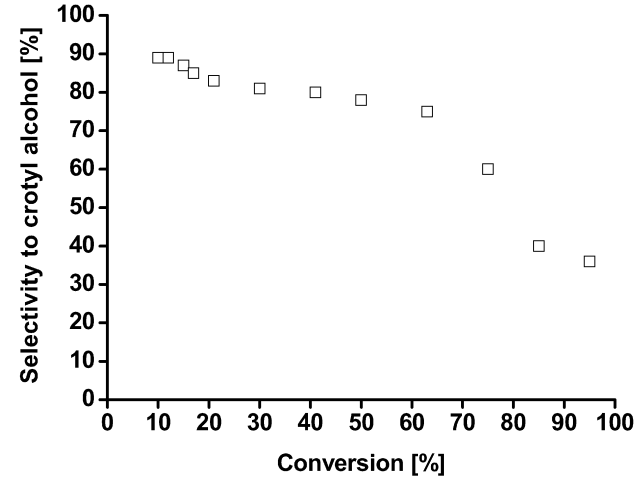

Fig. 8. Selectivity versus conversion for α5A (temp. red. = 300 °C, temp. reaction = 80 °C).

Table 3 compares our results with those reported in our previous studies of different catalytic systems [26,28–30] and studies published by others [22,32–37]. Bearing in mind that one must be very careful when comparing results presented of different studies due to unavoidable differences in catalyst preparation, experimental conditions, and other parameters, we believe that our results—especially those obtained on α5A catalyst—are exceptionally good and promising.

To throw more light on the special catalytic performance of some catalysts reported in this paper, we carried out physicochemical characterization using XRD, TPR, XPS, HRTEM and ToF-SIMS.

3.2. XRD

For our Ga_2O_3 sample, XRD patterns show characteristic lines at $2\theta = 24.5°$, 33.8°, 36.0°, 40.3°, 41.4°, 50.3°, 55.1°, 63.4° and 64.8°, corresponding to the diffractions (012), (104), (110), (006), (113), (024), (116), (214), and (300). These are in fact identical to those given in ICDS file (00-006-0503) and the literature [38], demonstrating that we are dealing with pure α-Ga_2O_3. Likewise, the commercial β-Ga_2O_3 shows characteristic lines according to ICDS file (01-076-0573). The mean crystallite sizes of α-Ga_2O_3 and β-Ga_2O_3 were estimated based on the broadening of XRD lines using Scherer's formula; these were ca. 16 nm and 22 nm, respectively. XRD patterns of the catalysts calcined at 200 °C and reduced at 100 and 300 °C related to the pure support are shown in Fig. 9. For catalyst β5A, both calcined and reduced, a broad line at 2θ about 39.8° is observed, which can be ascribed to the Pt(111) diffraction (ICDS 00-004-0802). In contrast to the β5A catalyst, XRD patterns of the β5H catalyst show a Pt(111) diffraction line for only the reduced samples. Indeed, in the calcined sample, platinum occurs in the form of oxychlorine species. The different intensities of samples reduced at 100 and 300 °C may suggest that the reduction of these catalysts at temperatures as low as 100 °C is not complete, as confirmed by TPR results. In addition, an increase in the reduction temperature may lead to an increase in platinum crystallites.

Interpretation of XRD patterns of the catalysts supported on α-Ga_2O_3 is more complex, because the reflex of α-Ga_2O_3 (006)

Table 3
Comparison of catalytic activities and selectivities for different Pt/support catalysts in selective hydrogenation of crotonaldehyde in a gaseous phase

Catalysts	Pretreatment (°C)	Reaction temperature (°C)	Steady-state activity	Selectivity to crotyl alcohol (%) (Cv < 20%)	Crotyl alcohol selectivity (%) (Cv > 50%)	Reference
Pt/Ga_2O_3	Red. 300	80	180[a] 0.1[b]	85–90	70	This paper
Pt/SnO_2	Red. 443 K	80	6[a]	70–75	50	[28]
Pt/ZnO	Red. 400	80	10[a] 0.006[b]	85–90	80	[26]
Pt/CeO_2	Red. 700 +calc. 400 K +rered. 500	80	10, 4[a] 0.006[b]	87		[29]
Pt/CeO_2-SiO_2	Red. 500	80	21[a] 68[a,c]	80		[32]
Pt-Sn/SiO_2	Red. 300	80	2.2[a,d]	70	60	[33]
Pt/TiO_2	Red. 400 +calc. 300 +rered. 200	80	100[a]	64		[34]
Pt/AC_{OX}		80	7[a]	35		[35]
$Pt/ZnCl_2/SiO_2$	Red. 400	80	6.5[a]	82		[30]
Pt/SiO_2	Red. 400	80	0.017[b]	5		[22]
Pt-Sn/SiO_2			0.029[b]	30, 5		
Pt-Ga/SiO_2			0.013[b]	49		
Pt-Bi/SiO_2			0.022[b]	6		
Pt-La/SiO_2			0.013[b]	7		
Pt-Pb/SiO_2			0.0053[b]	3		
$Pt/ZnO_2/TiO_2$	Red. 500	80	42[a]	50		[36]
Pt/TiO_2			34[a]	35		
Pt/SiO_2	Red. 500	80	95[a]	11	7	[37]
Pt-Sn/SiO_2			800[a]	59	50	

[a] Activity calculated as (μmol s^{-1} g_{Pt}^{-1}).
[b] Activity calculated as TOF (molec $site^{-1}$ s^{-1}).
[c] Calculated considering $E_a = 21$ kJ [33].
[d] Initial rate (μmol s^{-1} g_{Pt}^{-1}).

at $2\theta = 40.3°$ is almost in line with that coming from platinum. The only differences observed can be related to the broadening and intensities of lines, the trend of which is similar to that discussed for catalysts supported on β-Ga_2O_3.

3.3. TPR and TG–DTA–MS

TPR profiles of the catalysts are presented in Fig. 10. For the catalysts obtained from hexachloroplatinic acid (α5H and β5H), a large peak with a maximum at about 160 °C (α5H) and 200 °C (β5H) is observed. This peak can be assigned to the reduction of oxychlorine platinum species formed during preliminary drying and/or calcination of the catalysts precursor at 200 °C. A shift of the maximum toward lower temperatures in the case of the catalyst α5H may be due to better dispersion of oxychlorine species connected with the higher specific surface of α-Ga_2O_3. After termination of this peak, the hydrogen consumption is continued to about 800 °C. This can be attributed to the partial reduction of Ga_2O_3 promoted by metallic platinum occurring mainly on the catalyst surface. A two-stage character of this process can be seen. The diverse susceptibility to the reduction of the surface support species can be explained assuming that species being in the intimate contact with platinum are reduced more easily at lower temperatures, whereas those suffering due to a lack of metal–support contact need spilled-over hydrogen for reduction. It can be clearly seen that reduction of the support occurs in a significantly lower temperature range for the catalysts supported on α-Ga_2O_3, which have a much higher specific surface area compared with those supported on β-Ga_2O_3. In such a case, the intimate contact of platinum and Ga_2O_3 is preferential, due to better dispersion of metal on the surface.

TPR profiles of the catalysts prepared from the chlorine-free precursor $Pt(acac)_2$ do not contain the distinct low-temperature peaks. This means that either $Pt(acac)_2$ undergoes at least partial decomposition to metallic platinum during catalyst precalcination at 200 °C or/and PtO_x is reduced at room temperature before the start of TPR. PtO_x, especially in the form of large

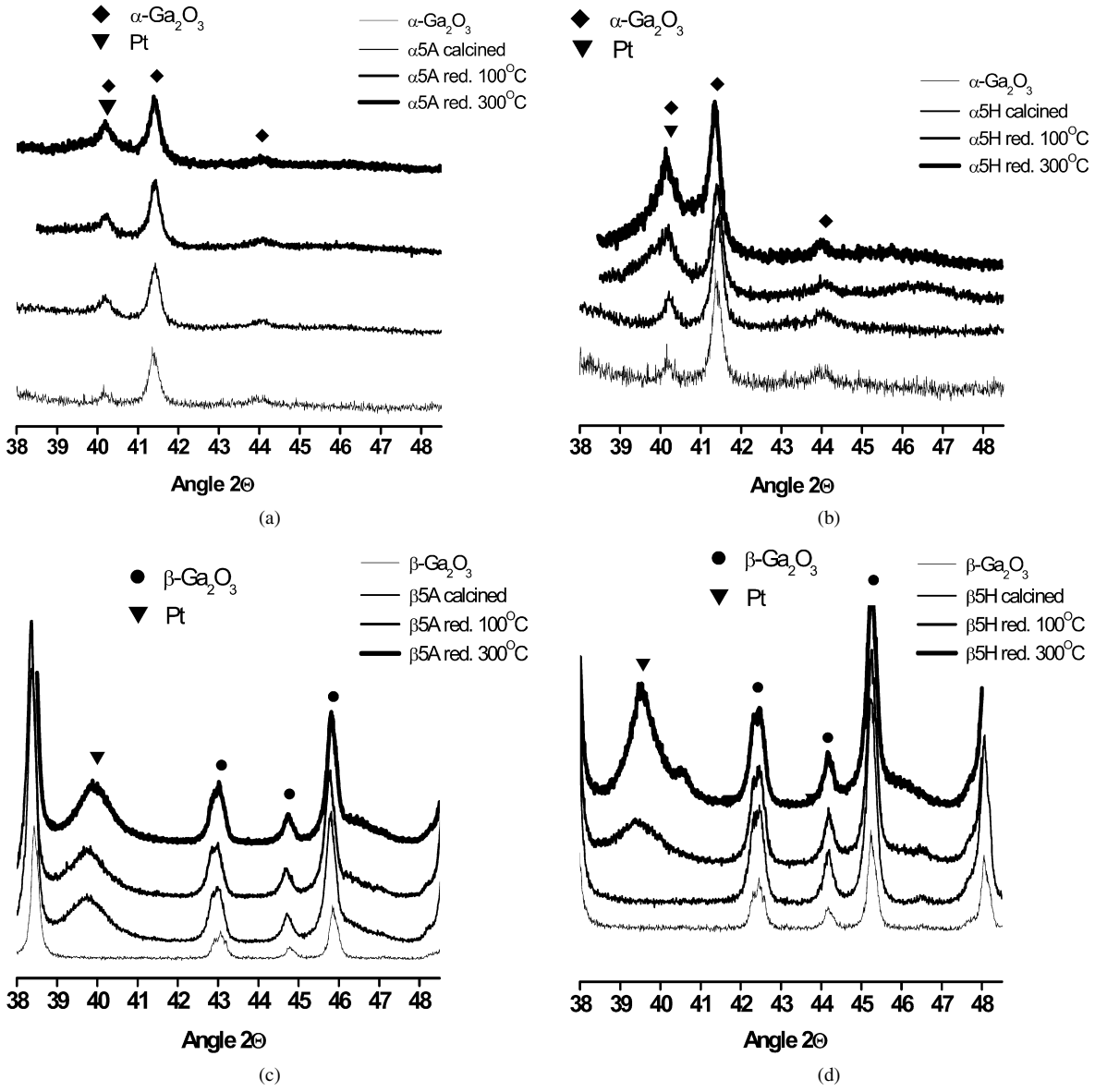

Fig. 9. XRD diffractograms of (a) α5A, (b) α5H, (c) β5A, (d) β5H.

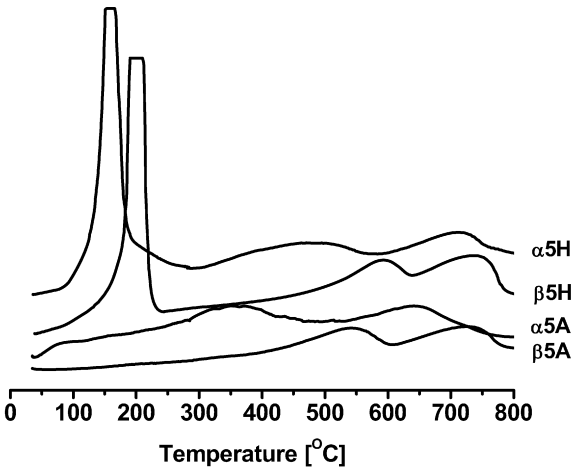

Fig. 10. TPR for 5 wt% catalysts.

crystallites, can be reduced at room temperature [39–41]. The ascending character of the TPR curves of catalysts α5A and β5A observed at very low temperatures (at the beginning of the TPR process at room temperature) may be connected with the further reduction of small platinum oxide crystallites, but also may indicate surface Pt-promoted support reduction. Until recently, it was believed that gallium oxide cannot be reduced by hydrogen below 600 °C [42]. However, Zheng et al. [38] showed that some part of Ga_2O_3 can be reduced at a low temperature (200–250 °C). The H_2:Ga_2O_3 molar ratio calculated by these authors is 0.1 for α-Ga_2O_3 and 0.045 for β-Ga_2O_3. Promoted by platinum, the surface reduction of gallia may occur at much lower temperatures.

Fig. 11 presents the thermal analysis of $Pt(acac)_2$ carried out in air atmosphere. The TG curve shows that the decomposition occurs directly to the metallic platinum, begins below 200 °C, and reaches a maximum at about 255 °C. Although the

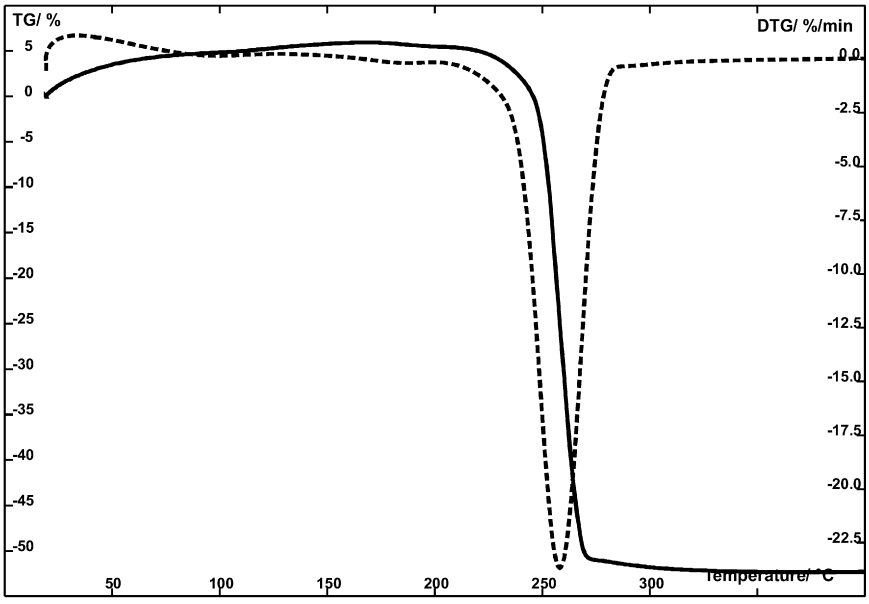

Fig. 11. TG–DTA–MS profile of $Pt(acac)_2$ decomposition.

temperature conditions of decomposition of pure and support deposited catalyst precursors are not always the same, the easiness of $Pt(acac)_2$ decomposition explains the occurrence of metallic platinum in the calcined catalysts prepared from this precursor.

3.4. HRTEM and ToF-SIMS measurements

Figs. 12–14 show examples of representative HRTEM images of some catalysts under study, both calcined at 200 °C and reduced at 100 and 300 °C. Based on these images, we estimated the distribution of platinum particles and the main size of platinum crystallites; the results are presented in Table 4.

Catalysts prepared from chlorine-free precursor α2A and α5A show high, homogeneous platinum dispersion, similar in both catalysts. An application of H_2PtCl_6 as an active-phase precursor leads to a significant increase in platinum crystallite size. The effect of chlorine on the nature of the catalysts and their activity and selectivity in the reaction of selective hydrogenation of α,β-unsaturated aldehydes is diversified and complex [19,26–29,31,43–45]. Residual chlorine can diminish the metal dispersion and enhance [26,27,46] or inhibit [31] formation of an alloy between platinum and metal originating from the reducible support. In the part of this paper describing catalytic properties of the studied catalysts, we showed that our Pt/Ga_2O_3 systems obtained from H_2PtCl_6 precursor are much less active, particularly due to the much larger platinum particles compared with those prepared from the chlorine-free precursor, although their selectivity was still high. That is why we focused our attention on such catalysts, especially α5A.

HRTEM images of the catalysts supported on α-Ga_2O_3 reveal a very interesting structure of this polymorphic modification. We can see a characteristic, hexagonal structure [47] of the cells. Relatively uniform platinum particles are regularly distributed in the center of the support cells. Thus, such a characteristic structure seems to "force" a regular distribution of platinum. As we demonstrated earlier, the best catalytic performance, taking into consideration both activity and selectivity to crotyl alcohol, is shown by catalyst α5A. As shown in Fig. 12, independent of the pretreatment of this catalyst (i.e., calcination at 200 °C and reduction at 100 and 300 °C), in all of these cases the particle sizes of platinum crystallites are similar within quite a narrow range (2–4.5 nm). The catalyst reduced at 300 °C shows significantly higher activity and selectivity to crotyl alcohol compared with that reduced at 100 °C, whereas the activity of the catalyst just calcined is minimal. Thus, it is obvious that the presence of metallic platinum, as well as crystallite size, influence the catalytic behavior of the catalyst under discussion. A careful analysis of the HRTEM pictures of the reduced samples, especially those reduced at 300 °C, seems to indicate the migration of partially reduced GaO_x on the top of platinum species, according to a well-known SMSI mechanism. To rationalize such a suggestion, we carried out SIMS investigations.

ToF-SIMS measurements were carried out for the catalysts reduced at 300 °C. Table 5 presents intensity ratios Pt^-/O^- on the surface of samples as prepared and after the removal of a few top monolayers. In all cases, the value of Pt^-/O^- was lower for subsurface regions. For catalysts α2A and α5A, this value dropped just 5.9- and 2.3-fold, respectively, whereas for catalysts β2A and β5A, 8.0- and 4.2-fold decreases were observed. The difference between the amount of Pt present on the surface and in the deeper layers is considerably smaller for Pt/α-Ga_2O_3. This probably means that Pt supported on β-Ga_2O_3 is situated mainly on top of the support surface, whereas in the second case, Pt crystallites are modified by a thin layer of partially reduced α-Ga_2O_3 and are situated slightly deeper in the subsurface region.

The prevailing opinion is that in crotonaldehyde hydrogenation, selectivity to the unsaturated alcohol increases with the

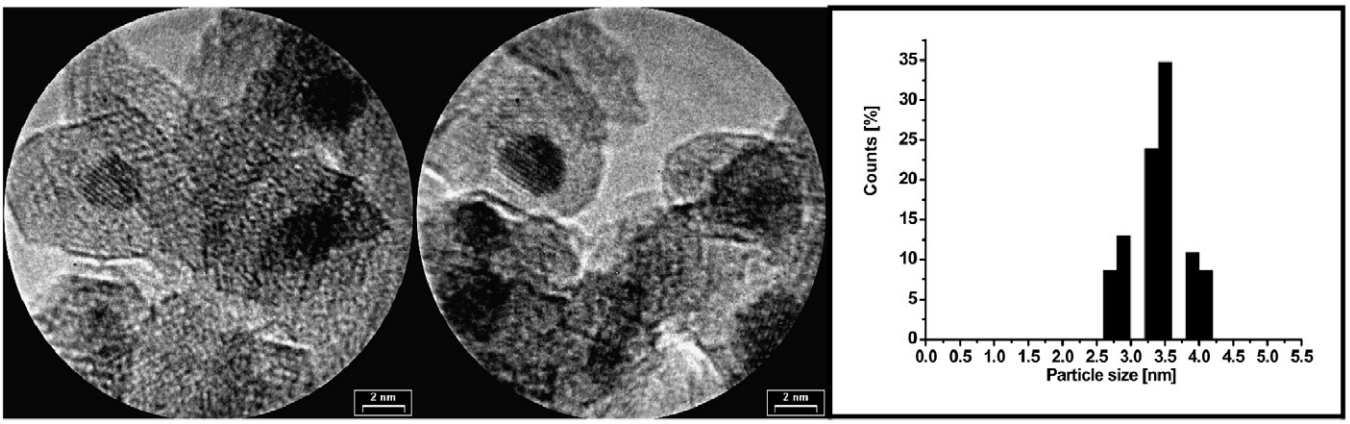

(a)

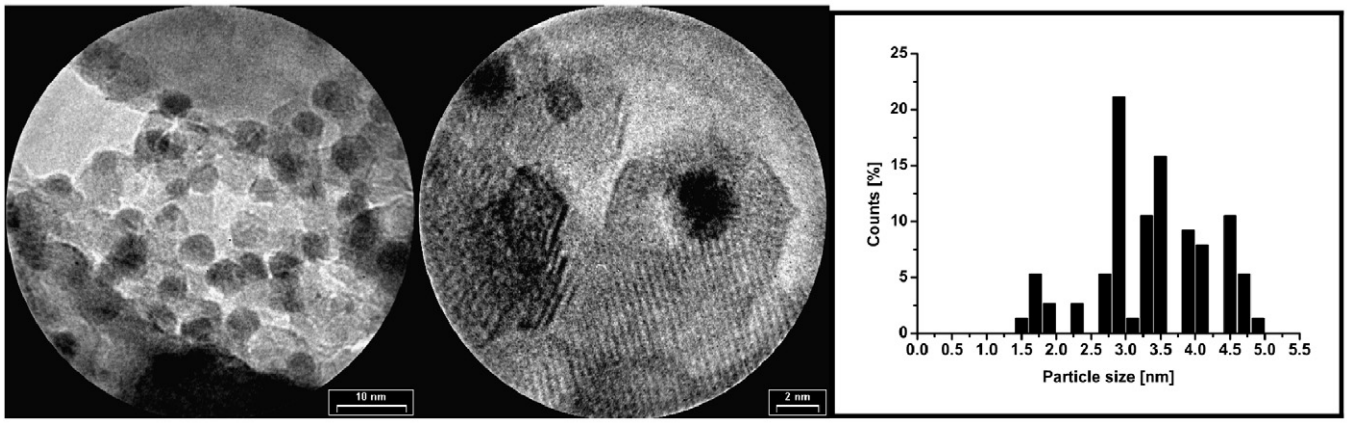

(b)

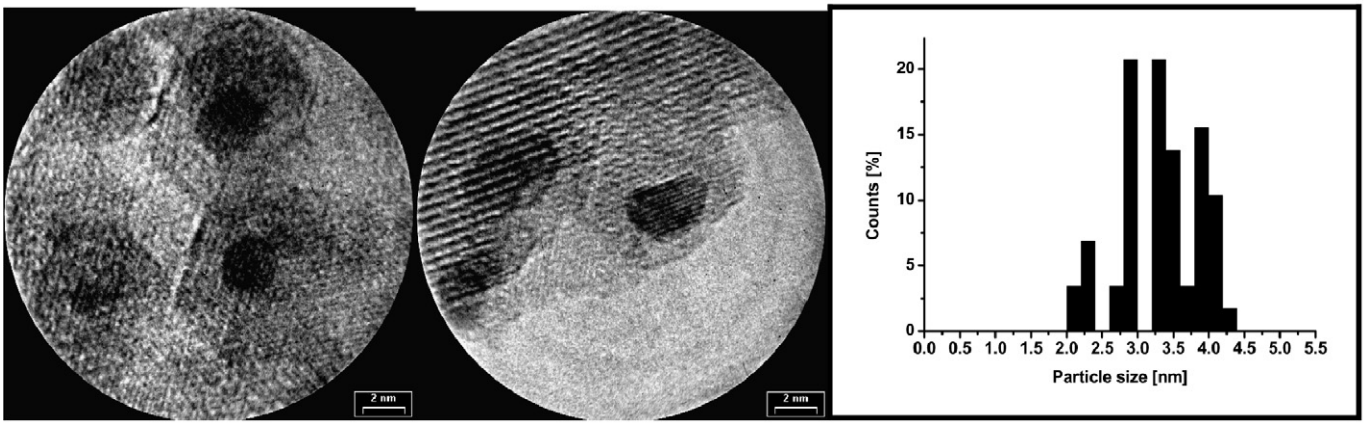

(c)

Fig. 12. HRTEM image and particle size histograms of α5A: (a) after calcination, (b) after reduction at 100 °C, (c) after reduction at 300 °C.

increase in metal particles [19]. Englisch et al. [48] concluded that in the case of large particles, the prevalent dense Pt(111) surface planes of Pt constrains sorption of the C=C double bond, which enhances the selectivity to hydrogenation of the carbonyl group. On the other hand, the abundance of highly exposed metal atoms in small particles favors an unrestricted sorption of both double bonds, facilitating hydrogenation of the C=C bond. However, only combined effects of metal particles nature and support and/or promoter interaction may improve the selectivity to a great extent. In the case of partly reducible supports, such as TiO_2, due to the SMSI effect, the presence of coordinatively unsaturated Ti atoms strengthens the interaction of catalyst with the C=O bond and thus enhances its hydrogenation. Englisch et al. stated that both the particle size and decoration of Pt particles by titania suboxides are additive effects, leading to increased selectivity. Other work has investigated a promoting effect of gallium in silica-supported platinum catalysts, improving the selectivity toward crotyl alcohol [22]. They suggest that gallium is present in the catalyst in the form of oxide electron pair acceptor sites, which activate

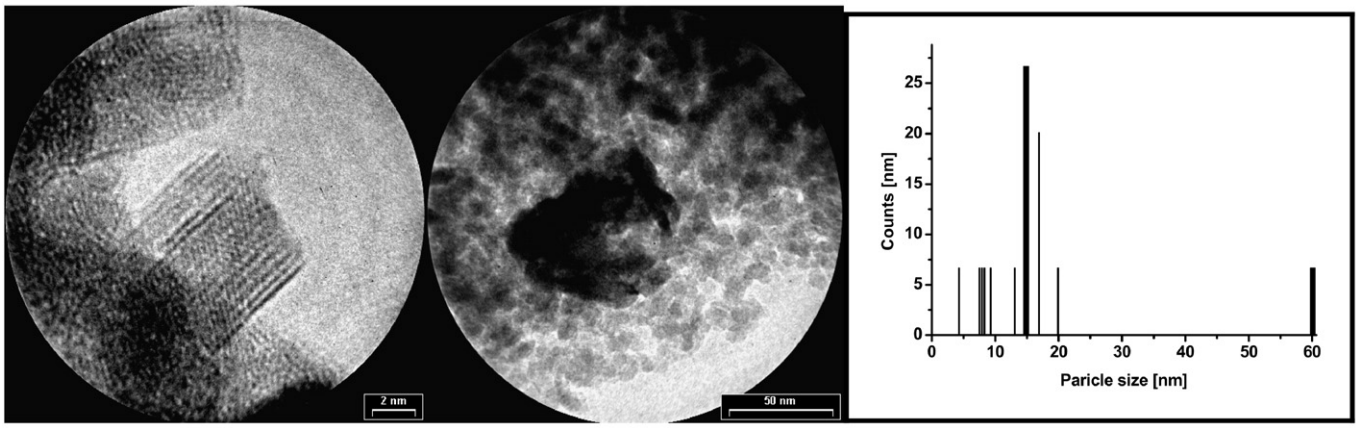

(a)

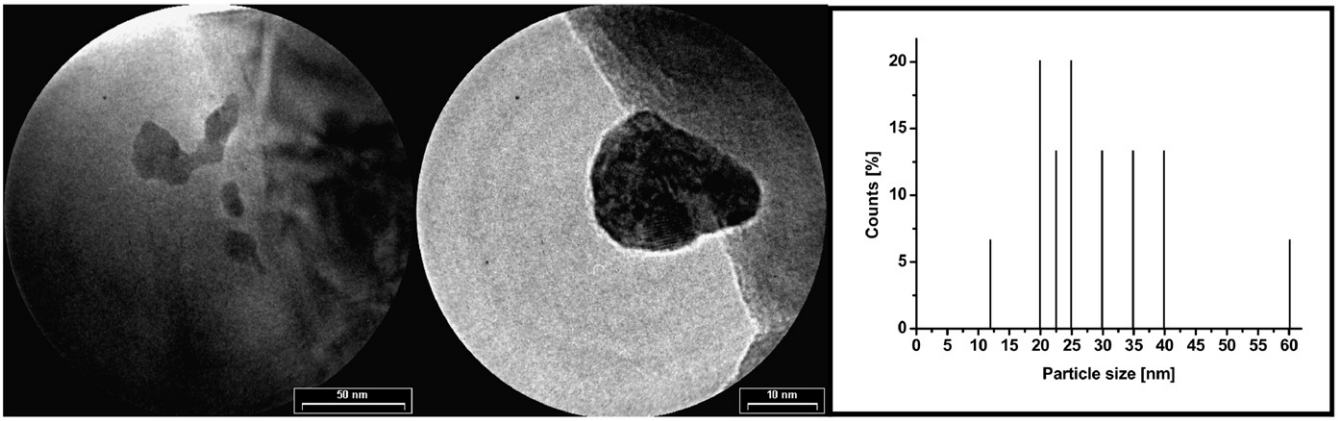

(b)

Fig. 13. HRTEM image and particle size histograms of: (a) α5H, (b) β5H.

the C=O bond by coordination to the oxygen of the carbonyl group.

In our studies, we demonstrated that gallium oxide is a partially reducible oxide. As a support, it behaved like TiO_2 decorating platinum particles with gallium suboxides. This effect is strengthened by a well-established promoting affect of gallium on the selectivity of carbonyl hydrogenation [5]. Another important factor contributing to the very high selectivity of the catalysts under study (especially catalyst α5A) is stabilization of the Pt dispersion by placing Pt particles in regular hexagonal cells of the α-Ga_2O_3 support.

3.5. Infrared spectroscopy

The FTIR analyses were carried out for α5A and β5A catalysts. The characteristic absorption bands of crotonaldehyde and CO were the same for both catalysts. Figs. 15 and 16 present FTIR spectra for α5A catalyst. IR spectroscopy of adsorbed carbon monoxide may be used to provide information on the size and morphology of metallic particles and the extent of interaction with the support [49,50]. Fig. 15 shows spectra obtained for the sample reduced at 300 °C and exposed to CO at 25 °C, which contain two broad absorption bands at 2065 and 1822 cm^{-1}. The first is assigned to linearly adsorbed CO on a single Pt^0 atom, whereas the second characterizes the CO bridged adsorption on two Pt atoms. The intensity and strength of the bridging band CO is very weak and hard to see [51]. This band disappears after a 10-min evacuation at room temperature, whereas the linear band is removed after outgassing at 100 °C.

For polyfunctional molecules, such as crotonaldehyde, several possible adsorption structures on the platinum catalysts surface can exist [50,52]:

- For adsorption through the C=C double bond, two structures are possible. These are designated $\pi_{CC}\eta_2$ and d_i-$\sigma_{CC}\eta_2$, corresponding to the adsorption band at 1641 and 1543, 1452 cm^{-1}, respectively;
- For adsorption through the C=O double bond, three structures are possible, ascribed as $\pi_{CO}\eta_2$, d_i-$\sigma_{CO}\eta_2$, and the η_1 "on-top" adsorption by an oxygen atom, corresponding to respective absorption bands at 1693, 1660, and 1680 cm^{-1};
- The structure where the adsorption occurs involves both double bonds, C=C and C=O, ascribed as η_4, with bands at 1693 and 1641 cm^{-1}.

The experimentally obtained FTIR spectra of adsorbed crotonaldehyde are presented in Fig. 16. Adsorption at room temperature resulted in the formation of absorption bands at 1718, 1683, 1614, 1440, 1371, and 1162 cm^{-1}. The intensity of the absorption bands at 1718, 1614, and 1440 cm^{-1} decreased after

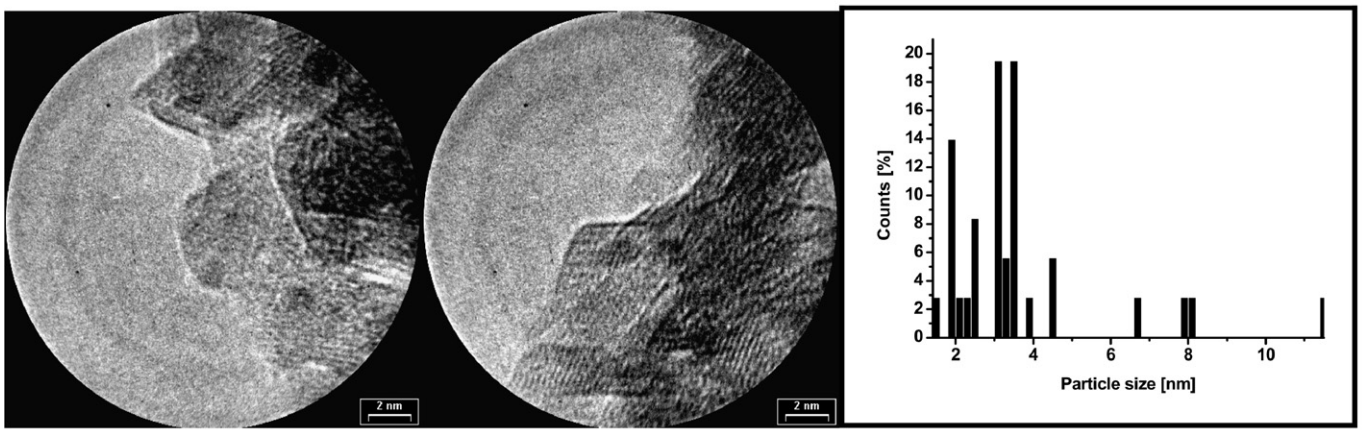

(a)

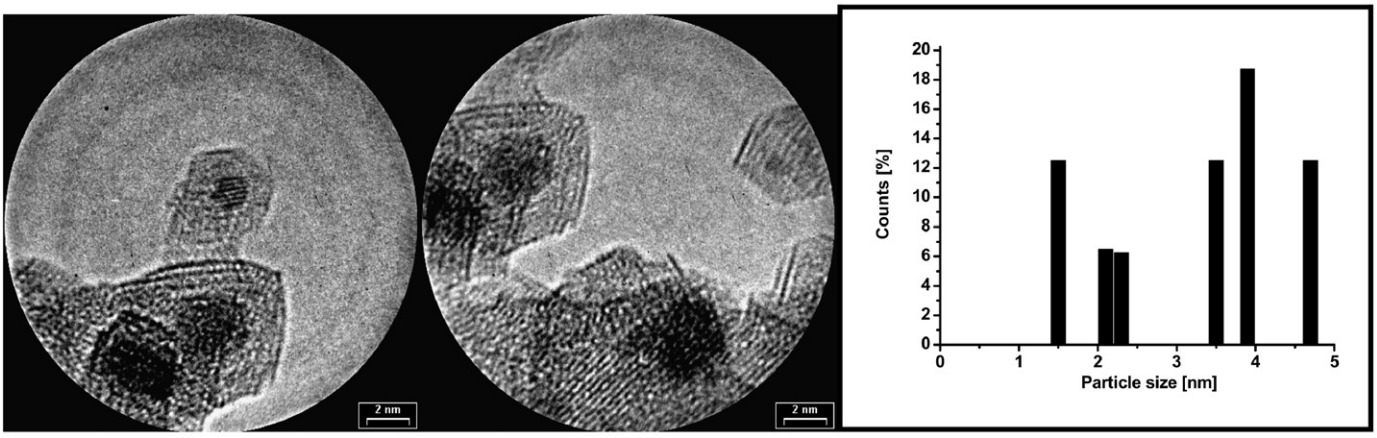

(b)

Fig. 14. HRTEM image and particle size histograms of α2A: (a) after reduction at 100 °C, (b) after reduction at 300 °C.

Table 4
Main size for platinum crystallites

Catalyst	α5A	α2A	α5H	β5A	β2A	β5H
Calc. 200 °C	3.4 nm	–	–	–	–	–
Red. 100 °C	2.8 nm	3.3 nm	–	–	–	–
Red. 300 °C	3.2 nm	3.7 nm	23.5 nm	10.9 nm	–	25.9 nm

Table 5
The values of Pt^-/O^- intensity ratios ($\times 10^3$) calculated for α2A, β2A, α5A, β5A catalysts after reduction at 300 °C

	α5A	α2A	β5A	β2A
(a) As prepared	2.5	3.6	14.0	12
(b) After removal a few top monolayers	1.1	0.61	3.3	1.5
a/b ratios	2.3	5.9	4.2	8

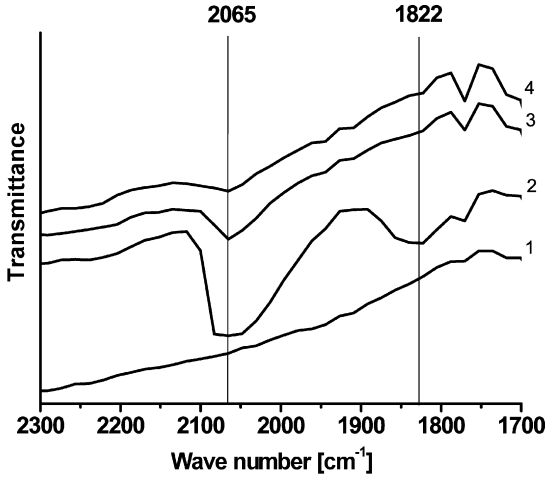

Fig. 15. FTIR spectra of CO on α5A: (1) "fresh" sample, (2) adsorption of CO at RT, (3) evacuation at RT, 10 min, (4) evacuation at RT, 30 min.

evacuation at room temperature. Because of the very close position of these bands to analogous ones in the crotonaldehyde gas phase, they can be assigned to $\nu_{C=O}$, $\nu_{C=C}$, and $\delta_{as}(CH_3)$ in the crotonaldehyde molecule. The absorption bands at 1683, 1371, and 1162 cm^{-1} remained in the spectrum after evacuation. These bands can be attributed to $\nu_{C=O}$, δ_{C-H}, and γ_{CH_3} vibrations in the coordinatively bonded crotonaldehyde, respectively. These results demonstrate that the molecules of crotonaldehyde are adsorbed on the catalyst surface by one platinum atom. The FTIR spectra show no absorption bands responsible for crotonaldehyde adsorption on the two Pt atoms (structures η_4, d_i-$\sigma_{CC}\eta_2$, and d_i-$\sigma_{CO}\eta_2$). This may suggest that platinum atoms have a close interaction with the support. Thus, FTIR analysis seems to confirm platinum decoration with a thin layer

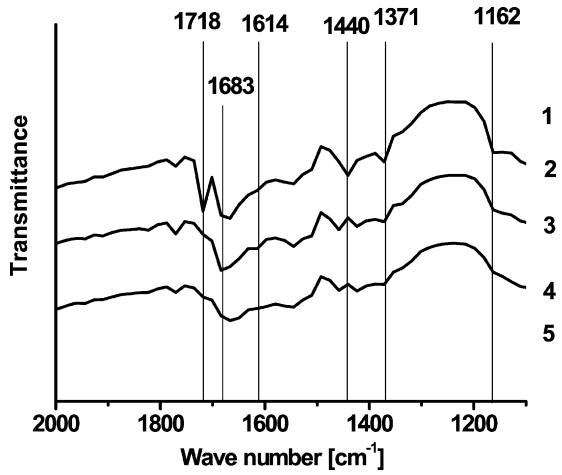

Fig. 16. FTIR spectra of C_4H_6O on α5A: (1) "fresh" sample, (2) adsorption of C_4H_6O at RT, (3) evacuation at RT, 10 min, (4) evacuation at RT, 30 min, (5) evacuated at 150 °C.

of a partially reduced support. In our spectra, only a band at 1683 cm^{-1} is observed, which can be attributed to the "on-top" η_1 position, connected with high catalyst selectivity in the hydrogenation of α,β-unsaturated aldehydes [50,52].

4. Conclusion

Platinum catalysts supported on gallium oxide appear to be very promising in the reaction of selective hydrogenation of crotonaldehyde to crotyl alcohol. The use of gallium oxide as a platinum support increases the C=O bond hydrogenation significantly while maintaining high activity, whereas Pt-based catalysts are usually reported with high selectivity but have poor activity. The best catalytic performance (high activity and selectivity) is given by the 5 wt% Pt/Ga_2O_3 catalyst prepared from the chlorine-free precursor: platinum acetylacetonate supported on α-Ga_2O_3. We have shown that the use of gallium oxide as a support for platinum increases the C=O bond hydrogenation selectivity considerably while maintaining high activity. These particular properties of Pt/α-Ga_2O_3 catalysts are due to the synergetic effect of the following advantages for selective hydrogenation of carbonyl group elements:

(a) surface reducibility of gallium oxide, leading to covering (decoration) of platinum by gallium suboxides;
(b) promoting effect of gallium;
(c) regular distribution of platinum particles on α-Ga_2O_3 by specific hexagonal structure of the support.

Acknowledgments

The authors thank Dr. Waldemar Maniukiewicz and Dr. Joanna Bojarska for XRD analysis. This work was supported by Grant 3 T09B 11326 (0112/T09/2004/26).

References

[1] R.L. Augustine, Heterogeneous Catalysis for the Synthetic Chemist, Dekker, New York, 1996.
[2] P.T. Anastas, L.B. Bartlett, M.M. Kirchhoff, T.C. Williamson, Catal. Today 55 (2000) 11.
[3] J. March, March's Advanced Organic Chemistry, McGraw–Hill Kogakusha, Tokyo, 1997, p. 829.
[4] V. Ponec, Appl. Catal. A 149 (1997) 27.
[5] S. Nishimura, Handbook of Heterogeneous Catalytic Hydrogenation for Organic Synthesis, Wiley, New York, 2001.
[6] P. Gallezot, D. Richard, Catal. Rev. Sci. Eng. 40 (1&2) (1998) 81.
[7] Y. Nitta, Y. Hiramatsu, T. Imanaka, J. Catal. 126 (1990) 235.
[8] Y. Nitta, K. Vero, T. Imanaka, Appl. Catal. A 56 (1989) 9.
[9] Y. Nitta, T. Kato, T. Imanaka, Stud. Surf. Sci. Catal. 78 (1993) 83.
[10] C. Ando, H. Kurokawa, H. Miura, Appl. Catal. 185 (1999) 181.
[11] M.B. Padley, C.H. Rochester, G.J. Hutchings, J. Catal. 148 (1994) 438.
[12] J.E. Bailie, C.H. Rochester, G.J. Hutchings, J. Chem. Soc. Faraday Trans. 93 (1997) 2331.
[13] J.E. Bailie, G.J. Hutchings, H.A. Abdullah, J.A. Anderson, C.H. Rochester, Phys. Chem. Chem. Phys. 2 (2002) 283.
[14] E.L. Rodrigues, J.M.C. Bueno, Appl. Catal. 232 (2002) 147.
[15] E.L. Rodrigues, A.J. Marchi, C.R. Apesteguia, J.M.C. Bueno, Stud. Surf. Sci. Catal. 130 (2000) 2087.
[16] E.L. Rodrigues, J.M.C. Bueno, Appl. Catal. 257 (2004) 201.
[17] F. Djerboua, D. Benachour, R. Touroude, Appl. Catal. 282 (2005) 123.
[18] A. Borgna, B.G. Anderson, A.M. Saib, H. Bluhm, M. Hävecker, A. Knop-Gericke, A.E.T. Kuiper, Y. Tamminaga, J.W. Niemantsverdriet, J. Phys. Chem. B 108 (2004) 17905.
[19] P. Mäki-Arvela, J. Hájek, T. Salmi, D.Yu. Murzin, Appl. Catal. A 292 (1&2) (2005) 1.
[20] T.B.L.W. Marinelli, S. Nabuurs, V. Ponec, J. Catal. 151 (1995) 431.
[21] A.B. da Silva, E. Jordão, M.J. Mendes, P. Fouilloux, Appl. Catal. A 148 (1997) 253.
[22] M. Englisch, V.S. Ranade, J.A. Lercher, J. Mol. Catal. A 121 (1997) 69.
[23] G. Neri, L. Mercadante, C. Milone, R. Pietropaolo, S. Galvano, J. Mol. Catal. A 108 (1996) 69.
[24] B. Coq, F. Figueras, Coord. Chem. Rev. 178–180 (1998) 1753.
[25] S.E. Collins, M.A. Baltanás, J.L. Garcia Fierro, A.L. Bonivardi, J. Catal. 221 (2002) 252.
[26] F. Ammari, J. Lamotte, R. Touroude, J. Catal. 221 (2004) 32.
[27] M. Consonni, D. Jokic, D.Yu. Murzin, R. Touroude, J. Catal. 188 (1999) 165.
[28] K. Liberková, R. Touroude, J. Mol. Catal. A 180 (2002) 221.
[29] M. Abid, G. Ehret, R. Touroude, Appl. Catal. 217 (2001) 219.
[30] F. Ammari, C. Milone, R. Touroude, J. Catal. 235 (2005) 1.
[31] M. Abid, R. Touroude, Catal. Lett. 69 (2000) 139.
[32] P. Concepcioń, A. Corma, J. Silvestre-Albero, V. Franco, J.Y. Chane-Ching, J. Am. Chem. Soc. 126 (2004) 5523.
[33] J.L. Margitfalvi, A. Tompos, I. Kolosova, J. Valyon, J. Catal. 174 (1998) 246.
[34] C. Raab, J.A. Lercher, Catal. Lett. 18 (1993) 99.
[35] F. Coloma, A. Sepulveda-Escribano, F. Rodríguez-Reinoso, Appl. Catal. A 123 (1995) L1.
[36] A.M. Ruppert, T. Paryjczak, Appl. Catal. A 320 (2007) 80.
[37] A.B. Merlo, G.F. Santori, J. Sambeth, G.J. Siri, M.L. Caselle, O.A. Ferretti, Catal. Commun. 7 (2006) 204.
[38] B. Zheng, W. Hua, Y. Yue, Z. Gao, J. Catal. 232 (2005) 143.
[39] D.E. Resasco, G.L. Haller, J. Catal. 82 (1982) 279.
[40] H. Lieske, G. Lietz, H. Spindler, J. Volter, J. Catal. 81 (1993) 8.
[41] F. Le Normand, A. Borgna, T.F. Garetto, R. Apesteguia, B. Moraweck, J. Phys. Chem. 100 (1996) 9068.
[42] M. Saito, S. Watanabe, I. Takahara, M. Inaba, K. Murata, Catal. Lett. 89 (3–4) (2003) 213.
[43] L.-P. Tiainen, P. Mäki-Arvela, A.K. Neyestanaki, T. Salmi, D.Yu. Murzin, React. Kinet. Lett. 78 (2003) 251.
[44] J. Hájek, N. Kumar, P. Mäki-Arvela, T. Salmi, D.Yu. Murzin, I. Paseka, T. Heikkilä, E. Laine, P. Laukkanen, J. Väyrynen, Appl. Catal. A 251 (2003) 385.
[45] B. Bachiller-Baeza, A. Guerrero-Ruiz, I. Rodríguez-Ramos, Appl. Catal. A 192 (2000) 289.
[46] J. Silvestre-Albero, F. Coloma, A. Sepúlveda-Escribano, F. Rodriguez-Reinoso, Appl. Catal. A 304 (2006) 159.

[47] R. Roy, V.G. Hill, E.F. Osborn, J. Am. Chem. Soc. 74 (1952) 710.
[48] M. Englisch, A. Jentys, J.A. Lercher, J. Catal. 166 (1997) 25.
[49] F. Coloma, J.M. Coronado, C.H. Rochester, J.A. Anderson, Catal. Lett. 51 (1998) 155.
[50] F. Delbecq, P. Sautet, J. Catal. 152 (1995) 217.
[51] P. Bazin, O. Saur, J.C. Lavalley, M. Daturi, G. Blanchard, Phys. Chem. Chem. Phys. 7 (2005) 187.
[52] A. Dandekar, M.A. Vannice, J. Catal. 183 (1999) 344.